

lattice relaxation for neutral and charged defects.

We thank M. Altarelli, O. K. Andersen, S. T. Pantelides, and M. Schlüter for critically reading the manuscript. Two of us (J.P.V. and G.B.B.) gratefully acknowledge the warm hospitality of the Physikalisch-Technische Bundesanstalt in Braunschweig where part of this work was done.

<sup>(a)</sup>Permanent address.

<sup>1</sup>M. Scheffler, in *Festkörperprobleme: Advances in Solid State Physics*, edited by P. Grosse (Vieweg, Braunschweig, 1982), Vol. 22.

<sup>2</sup>M. Jaros, *Adv. Phys.* **29**, 409 (1980).

<sup>3</sup>G. A. Baraff, E. O. Kane, and M. Schlüter, *Phys. Rev. B* **25**, 548 (1982).

<sup>4</sup>D. Vanderbilt and J. D. Joannopoulos, *Phys. Rev. Lett.* **49**, 823 (1982).

<sup>5</sup>J. Bernholc, N. O. Lipari, and S. T. Pantelides, *Phys. Rev. B* **21**, 3545 (1980).

<sup>6</sup>G. A. Baraff and M. Schlüter, *Phys. Rev. B* **19**, 1965 (1979).

<sup>7</sup>An alternative way would be to determine the equilibrium distortion from the minimum of the total energy. This, however, involves a more elaborate calculation, because the total energy contains *explicitly* the corrections due to many electron interactions.

<sup>8</sup>A detailed description of the theory and its application to GaP:C<sub>Ga</sub>, :Ge<sub>Ga</sub>, and :Si<sub>Ga</sub> will be published elsewhere.

<sup>9</sup>R. P. Feynman, *Phys. Rev.* **56**, 340 (1939).

<sup>10</sup>It is well known from molecular calculations that a basis set  $\{\varphi_{\alpha}\}$  which is appropriate for electronic structure calculations is usually not sufficiently complete for a calculation of the force. However, the inclusion of the functions  $d\varphi_{\alpha}/dq$  in the basis set implies that the calculated force comes to close agreement with the slope of the total energy [see H. Nakatsuji, K. Kanda, and T. Yonezawa, *Chem. Phys. Lett.*

**75**, 340 (1980)]. For *s-p*-bonded impurities studied in the present paper we have therefore included also *d* and *f*<sub>0</sub> basis functions (see also Ref. 8). Furthermore, it is worth noting that pseudopotential force calculations do not suffer from core polarization effects since the differentiation of the Hamiltonian is performed after the frozen-core approximation is made [see J. Harris, R. O. Jones, and J. E. Müller, *J. Chem. Phys.* **75**, 3904 (1981)].

<sup>11</sup>M. Scheffler, S. T. Pantelides, N. O. Lipari, and J. Bernholc, *Phys. Rev. Lett.* **47**, 413 (1981), and to be published.

<sup>12</sup>F. Mehran, T. N. Morgan, R. S. Title, and S. E. Blum, *Solid State Commun.* **11**, 661 (1972).

<sup>13</sup>P. J. Dean, W. Schairer, M. Lorenz, and T. N. Morgan, *J. Lumin.* **9**, 343 (1974).

<sup>14</sup>M. R. Lorenz, G. D. Pettit, and S. E. Blum, *Solid State Commun.* **10**, 705 (1972).

<sup>15</sup>A. T. Vink, R. L. A. Van der Heyden, and J. A. W. Van der Does de Bye, *J. Lumin.* **8**, 105 (1973).

<sup>16</sup>M. Altarelli, *J. Phys. Soc. Jpn.* **49**, Suppl. A, 169 (1980).

<sup>17</sup>D. R. Hamann, M. Schlüter, and C. Chiang, *Phys. Rev. Lett.* **43**, 1494 (1979); G. B. Bachelet, D. R. Hamann, and M. Schlüter, *Phys. Rev. B* **26**, 4199 (1982).

<sup>18</sup>The use of local pseudopotentials, which give a reasonable bulk charge density, is appropriate for the host ions. This can be understood in particular at the undistorted geometry: Here the electronic contribution to  $F^0$  (which depends very sensitively on the host crystal restoring forces) vanishes by symmetry. Therefore the only way these potentials enter our force is through their ability to provide a good description of the change in the electronic structure induced by the defect. This ability was well established previously (Ref. 11).

<sup>19</sup>The Coulombic tail that is present in the potential of the transition-state calculation was included by perturbation theory.

## Calculated Structural Phase Transitions in the Alkaline Earth Metals

Hans L. Skriver

*Risø National Laboratory, DK-4000 Roskilde, Denmark*

(Received 21 September 1982)

The local-density approximation and the linear muffin-tin orbital method have been used within the atomic-sphere approximation to calculate structural energy differences for all the alkaline earth metals at zero temperature. At ordinary pressure the calculations predict the crystal structure sequence hcp→fcc→bcc as a function of atomic number. As a function of pressure they predict the structure sequence fcc→bcc→hcp. The structural transitions and the onset of superconductivity under pressure are correlated with the *d* occupation number.

PACS numbers: 64.70.Kb, 61.50.+t, 61.60.+m, 62.50.+p

The crystal structures of the elemental metals tend to occur in certain sequences, both as a function of atomic number and as a function of

pressure. Most celebrated in this respect are the hcp→Sm-type→dhcp→fcc and the hcp→bcc→hcp→fcc sequences observed in the rare-earth

and the transition-metal series, respectively. The most recent explanations<sup>1</sup> from first principles for these two sequences have been based upon canonical band calculations<sup>2</sup> which establish a strong correlation between the occurrence of a given crystal structure and the  $d$  occupation number.

The alkaline earth metals have a crystal-structure sequence of their own, i.e., hcp-fcc-bcc, as a function of atomic number. An attempt to understand the fcc-bcc part of this sequence based upon pseudopotential theory<sup>3</sup> explained the bcc structure in Ba and the pressure- (and temperature-) induced fcc-bcc transition in Sr, but gave the incorrect (bcc) zero-pressure crystal structure in Ca. In addition, later pseudopotential calculations<sup>4</sup> indicated that within this approach the stable structure at ordinary pressure should be the fcc structure for all the alkaline earths. Hence, it is still a challenge to the theory of electronic states to predict the crystal structures of the alkaline earth metals as a function of both atomic number and pressure.

In this paper I present a series of first-principles calculations of the electronic contribution to the structural energy differences for the alkaline earth metals, Be, Mg, Ca, Sr, Ba, and Ra, plus the divalent rare earths, Eu and Yb. The theory predicts in all cases the correct crystal structure at ordinary pressure and low temperature, except for Yb where the fcc structure is found to be marginally more stable than the experimentally observed hcp structure. As a function of increasing pressure the theory predicts the sequence fcc-bcc-hcp for Ca, Sr, and Yb and bcc-hcp for Eu and Ba. All but one of the transitions involved are expected to occur in the pressure range below 60 GPa, and they are therefore accessible to experimental verification.

The structural energy differences were calculated within the local density approximation<sup>5</sup> simply as the differences between the appropriate sums of the one-electron energies. Since it is not yet widely appreciated that this is an extremely accurate approximation I shall now describe the steps which lead to the procedure. For a given metal at a given atomic volume I solve the energy band problem self-consistently,<sup>6</sup> assuming an fcc crystal structure. Thereby I have minimized the energy functional,  $U\{n\}$ , with respect to changes in the electron density,  $n$ , and have obtained the ground-state density,  $n_{fcc}^{sc}$ . In a brute-force calculation one should now perform a similar calculation assuming,

say, a bcc structure, and subtract to find the structural energy difference

$$\Delta_{bcc-fcc} = U_{bcc}\{n_{bcc}^{sc}\} - U_{fcc}\{n_{fcc}^{sc}\}. \quad (1)$$

However, because of the stationary properties of  $U$  we may to a good approximation obtain  $U_{bcc}$  from a trial charge density,  $n_{bcc}^{tr}$ , which differs slightly from  $n_{bcc}^{sc}$ . This trial charge density I construct by positioning self-consistent fcc atomic-sphere potentials in a bcc geometry, solving the corresponding one-electron Schrödinger equation, and populating the lowest-lying one-electron states. Hence,

$$\Delta_{bcc-fcc} = U_{bcc}\{n_{bcc}^{tr}\} - U_{fcc}\{n_{fcc}^{sc}\}, \quad (2)$$

where the errors relative to Eq. (1) are of second order in  $n_{bcc}^{tr} - n_{bcc}^{sc}$ . Now, the use of a frozen, i.e., not self-consistently relaxed, potential to generate  $n_{bcc}^{tr}$  ensures that the chemical shifts in the core-electron energies drop out of Eq. (2) and also that the double counting terms cancel. This is in the spirit of the force relation.<sup>7,8</sup> For an elemental metal there is no electrostatic interaction between the Wigner-Seitz spheres in the atomic-sphere approximation and we are therefore led to consider only the sum of the one-electron energies for the valence electrons, i.e.,

$$\Delta_{bcc-fcc} = \int^{E_F} EN_{bcc}(E)dE - \int^{E_F} EN_{fcc}(E)dE, \quad (3)$$

where  $N(E)$  is the one-electron state density. The atomic-sphere approximation<sup>6</sup> is ideally suited for our purpose since it separates the potential- and crystal-structure-dependent parts of the energy band problem. Hence, all that is required at a given atomic volume, in addition to the self-consistent fcc calculation, is to calculate the energy bands in the bcc (or hcp) structure with use of the self-consistent fcc potential parameters, evaluate the sums of the one-electron energies, and subtract according to Eq. (3). This procedure is quite general, treats all  $s$ ,  $p$ ,  $d$ , (and  $f$ ) electrons on the same footing, and may be applied to all metals in the periodic table.

The sum of the one-electron energies has been calculated using the LMTO-ASA<sup>6</sup> method for the alkaline earth metals in the closely packed crystal structures, fcc, bcc, and hcp ( $c/a=1.57$ ) over a range of atomic volume. The resulting structural energy differences evaluated at the experimentally observed equilibrium lattice spacings are plotted in Fig. 1. The values for Mg are similar

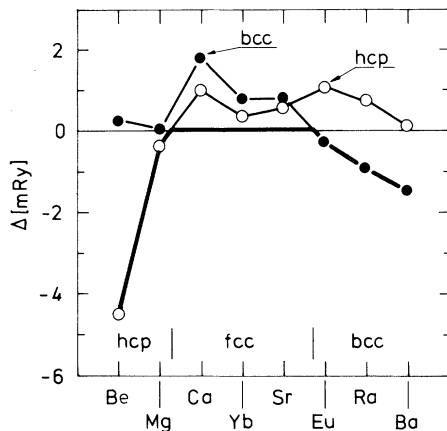


FIG. 1. Calculated structural energy differences for the alkaline earth metals in the three closely packed crystal structures, hcp, fcc, and bcc, evaluated at the observed equilibrium atomic volume, and plotted relative to the fcc phase. The metals are ordered according to their calculated  $d$  occupation number.

to those found in a recent total-energy calculation.<sup>9</sup> According to the results in Fig. 1 Be and Mg should form in the hcp structure, Ca and Sr in the fcc structure, and Ra and Ba in the bcc structure in complete agreement with experimental observations.

In Fig. 2 I have plotted the calculated pressure and the stable crystal structures as functions of the calculated  $d$  occupation number. Since no adjustable parameters have been used to construct the figure it is very satisfactory to note that all the zero-pressure crystal structures are given correctly by the theory, except for the case of Yb where the fcc structure is predicted. However, at an increased volume, 3% above the measured equilibrium volume, the hcp phase is calculated to be the stable phase, and hence one may not have to invoke zero-point motion in order to explain the anomalous, experimentally observed low-temperature hcp phase in Yb.

Under pressure the  $s$  electrons become trapped between the core from which they are excluded by orthogonality requirements and the decreasing atomic volume.<sup>1</sup> They respond by increasing their kinetic energy whereby the  $s$  band rises relative to the  $d$  band and  $s$  electrons are transferred into the  $d$  band. At the same time the hybridization gap at the Fermi level which stabilizes the fcc structure develops into a genuine gap and the fcc metal turns into a semiconductor.<sup>10</sup> The gap will close again at high pressure but shortly before this happens the bcc phase is calculated

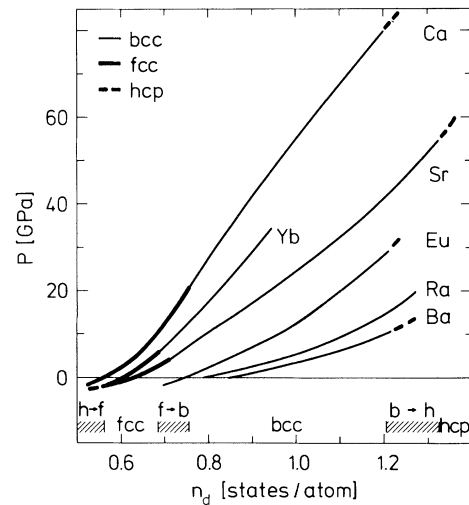


FIG. 2. Calculated crystal structures as a function of the  $d$  occupation number,  $n_d$ , and pressure,  $P$ . The hatched areas at the bottom of the figure indicate the  $n_d$  ranges within which the structural phase transitions are calculated to occur.

to be stable and the semiconducting behavior terminated. The calculated pressure range for the semiconducting phase is found to be 7–21, 0.3–4, and 0–6 GPa for Ca, Sr, and Yb, respectively, in reasonable agreement with high-pressure resistivity data.<sup>11–16</sup>

It follows from Fig. 2 that the individual metals at zero pressure may be characterized as being at different stages on the continuous  $s$ -to- $d$  transition, i.e., by their  $d$  occupation number. Furthermore, since the electronic structures of the metals included are very similar it is perhaps not so surprising that also the structural phase transitions, e.g., fcc  $\rightarrow$  bcc, correlate with the relative position of the  $s$  and  $d$  bands as already noted by Mackintosh and Andersen.<sup>9</sup> In fact, it is this correlation which is behind the single  $f$  parameter used by Johansson and Rosengren<sup>4,17</sup> to explain trends among the rare earths and neighboring elements. The correlation is, however, not completely perfect, and the calculated crystal-structure changes occur over a (narrow) range of  $d$  occupation numbers. The critical pressures for the fcc  $\rightarrow$  bcc transition in Sr and Yb plus the bcc  $\rightarrow$  hcp transition in Ba are found to be in good agreement with the low-temperature extrapolation of the high-pressure crystallographic measurements,<sup>18–20</sup> i.e., 4, 5, and 5 GPa, respectively. It should be possible to verify the predicted fcc  $\rightarrow$  hcp transition in Ca and Sr by present-day high-pressure techniques. The bcc

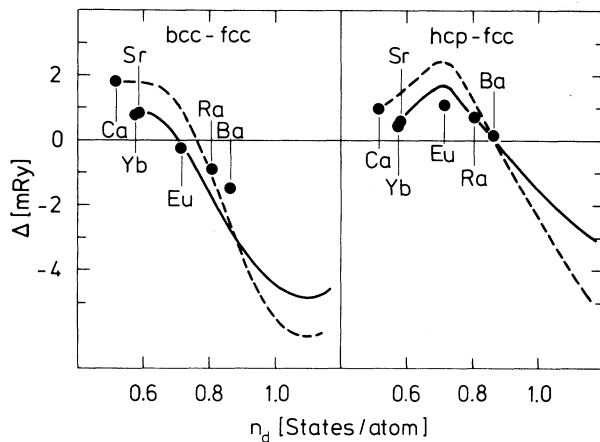


FIG. 3. Calculated structural energy differences relative to the fcc phase as functions of  $d$  occupation number for Sr, full lines, and Ca, broken lines. The full circles indicate the calculated values at the observed equilibrium atomic volume.

→ hcp transition expected above 30 GPa in Eu will probably not occur because Eu at this pressure will have changed valence<sup>17,21</sup> and taken up one of the crystal structures characteristic of the trivalent lanthanides. Ra is not found to transform into the hcp structure in the  $d$  occupation number range considered but may do so at higher compression.

If we assume that the onset of superconductivity under pressure is governed also by the  $d$  occupation number and accept the value<sup>15</sup> of 45 GPa for this transition in Ca we find from Fig. 2 that Yb, Sr, and Ba should be superconducting for  $n_d$  larger than 0.92, i.e., in the range above 31, 18, and 1 GPa, respectively, in good agreement with high-pressure conductivity measurements<sup>16</sup> for Sr and Ba. From Fig. 2 one may therefore conclude that Ra, if measured at high pressures, should be superconducting above 2.5 GPa.

The close similarity among the alkaline earth metals plus Eu and Yb is reflected in Fig. 3 where the calculated structural energy differences at normal volumes are found to group around the Sr curve. The Ca results deviate somewhat from this regularity presumably because this element, unlike the rest, has no  $d$  core. One also notes another irregularity in this figure, as well as in Fig. 2, namely that Ra at equilibrium has fewer  $d$  electrons than Ba, a result that must be due to the fact that Ra is the first element in the row which has an  $f$  core. It may finally be seen that if Ca, Yb, and Sr plus perhaps Eu, Ra, and Ba could be expanded they should eventually trans-

form into the hcp structure which is established experimentally as the low-temperature phase in Yb.

I wish to thank B. Johansson for pointing out the correlation between superconductivity and  $d$  occupation as well as for many fruitful discussions. This work was supported by the Danish Natural Science Research Council.

<sup>1</sup>J. C. Duthie and D. G. Pettifor, Phys. Rev. Lett. **38**, 564 (1977); D. G. Pettifor, in *Metallurgical Chemistry*, edited by O. Kubaschewski (Her Majesty's Stationery Office, London, 1972); D. G. Pettifor, CALPHAD **1**, 305 (1977).

<sup>2</sup>O. K. Andersen, J. Madsen, U. K. Poulsen, O. Jepsen, and J. Kollar, Physica (Utrecht) **86-88B**, 249 (1977).

<sup>3</sup>A. O. E. Animalu, Phys. Rev. **161**, 445 (1967).

<sup>4</sup>J. A. Moriarty, Phys. Rev. B **8**, 1338 (1973).

<sup>5</sup>W. Kohn and L. J. Sham, Phys. Rev. **140A**, 1135 (1965); L. Hedin and B. I. Lundqvist, J. Phys. C **4**, 2064 (1971); B. von Barth and L. Hedin, J. Phys. C **5**, 1629 (1972).

<sup>6</sup>The energy-band calculations employed the linear muffin-tin orbital (LMTO) method including the correction to the atomic-sphere approximation (ASA) [see O. K. Andersen, Phys. Rev. B **12**, 3060 (1975)], and included  $s$ ,  $p$ , and  $d$  partial waves. The electron density of the appropriate cores were frozen and the relativistic shifts included, but spin-orbit coupling was neglected.

<sup>7</sup>R. M. Nieminen and C. H. Hodges, J. Phys. F **6**, 573 (1976); D. G. Pettifor, Commun. Phys. **1**, 141 (1977).

<sup>8</sup>A. R. Mackintosh and O. K. Andersen, in *Electrons at the Fermi Surface*, edited by M. Springford (Cambridge Univ. Press, Cambridge, New York, 1980); O. K. Andersen, H. L. Skriver, H. Nohl, and B. Johansson, Pure Appl. Chem. **52**, 93 (1979).

<sup>9</sup>J. A. Moriarty and A. K. McMahan, Phys. Rev. Lett. **48**, 809 (1982).

<sup>10</sup>J.-P. Jan and H. L. Skriver, J. Phys. F **11**, 805 (1981).

<sup>11</sup>R. A. Stager and H. G. Drickamer, Phys. Rev. **131**, 2524 (1963).

<sup>12</sup>R. A. Stager and H. G. Drickamer, Science **139**, 1284 (1963).

<sup>13</sup>P. C. Souers and G. Jura, Science **140**, 481 (1963).

<sup>14</sup>D. B. McWhan, T. M. Rice, and P. H. Schmidt, Phys. Rev. **177**, 1063 (1969).

<sup>15</sup>K. J. Dunn and F. P. Bundy, Phys. Rev. B **24**, 1643 (1981).

<sup>16</sup>F. P. Bundy and K. J. Dunn, in *Physics of Solids Under High Pressure*, edited by J. S. Schilling and R. N. Shelton (North-Holland, Amsterdam, 1981).

<sup>17</sup>B. Johansson and A. Rosengren, Phys. Rev. B **11**, 2836 (1975).

<sup>18</sup>A. Jayaraman, Phys. Rev. **135**, A1056 (1964).

<sup>19</sup>A. Jayaraman, W. Klement, Jr., and G. C. Kennedy, Phys. Rev. **132**, 1620 (1963).

<sup>20</sup>A. Jayaraman, W. Klement, Jr., and G. C. Kennedy,

Phys. Rev. Lett. **10**, 387 (1963).

<sup>21</sup>A. Rosengren and B. Johansson, Phys. Rev. B **13**, 1468 (1976).

## X-Ray Diffraction Study of Electronic Transitions in Cesium under High Pressure

K. Takemura<sup>(a)</sup> and S. Minomura

*The Institute for Solid State Physics, The University of Tokyo, Roppongi, Minato-ku, Tokyo 106, Japan*

and

O. Shimomura

*National Institute for Research in Inorganic Materials, Sakura-mura, Niihari-gun, Ibaraki 305, Japan*

(Received 12 March 1982)

The crystal structure of the high-pressure phase of cesium (IV) was determined to be a tetragonal lattice with  $Z = 4$ . The space group is  $D_{4h}^{19}-I4_1/amd$  and the lattice parameters are  $a = 3.349 \text{ \AA}$  and  $c = 12.487 \text{ \AA}$  at 8.0 GPa. From the structure it is deduced that the atomic radius of cesium decreases dramatically at the III-IV transition, which suggests a discontinuous  $s-d$  electronic transition.

PACS numbers: 61.55.Fe, 64.70.Kb

Cesium is well known to show many polymorphic transitions under pressure. The crystal structure of Cs, which is bcc at normal pressure, changes to fcc (Cs II) at 2.3 GPa and to another fcc (Cs III) at 4.2 GPa.<sup>1</sup> The transition from Cs II to Cs III is a rare case of isomorphous transitions. It goes further to Cs IV at 4.3 GPa<sup>1,2</sup> and Cs V at about 10 GPa.<sup>3,4</sup> The characteristic behavior of Cs under pressure is interpreted in terms of  $s-d$  electronic transition. At normal pressure, the conduction band of Cs is almost of  $s$  character, but the lowest  $5d$  band including the  $X_1$  state already touches the Fermi level. As pressure is increased, the  $5d$  subbands near the  $X$  point go down relative to the  $6s$  band near the  $\Gamma$  point.<sup>5,6</sup> As the  $X_1$  subband has the same symmetry as the  $6s$  band, there occurs hybridization between the two bands. The movement of the  $X_1$  subband downwards in energy with pressure facilitates the electron transfer from the  $6s$  band to the more localized  $5d$  band. This causes the unusually soft bulk modulus in the low-pressure region (phases I and II).<sup>7</sup> On the other hand, the isostructural II-III transition is related to the higher energy  $5d$  states of  $X_3$  symmetry.<sup>6</sup> These states do not have the right symmetry to hybridize with the  $6s$  band and therefore the  $X_3$  subband abruptly shifts down through the Fermi level with increasing pressure. Recent relativistic calculation of pressure isotherms of Cs shows that the isostructural transition does not occur at  $T=0$  and that the thermal effect plays an important role in the transition at room temperature.<sup>8</sup> This calculation well accounts for the

disappearance of the II-III transition at low temperature<sup>9</sup> and the dramatic fall of melting temperature with pressure of Cs II.<sup>10</sup>

Band calculations<sup>5</sup> suggest that the electronic transition continues to take place to about 10 GPa. Therefore it is important to establish the crystal structure of phase IV, to gain an understanding of the nature of the  $s-d$  transition. The structure determination of Cs IV has been tried by Hall, Merrill, and Barnett<sup>1</sup> and by Inoue<sup>11</sup> using the x-ray diffraction technique and by McWhan, Bloch, and Parisot using the neutron diffraction technique.<sup>12</sup> Their results were, however, not sufficient to determine the structure. We have carried out high-pressure powder x-ray diffraction analysis on Cs IV utilizing a diamond-anvil cell<sup>13</sup> and an x-ray position-sensitive detector.<sup>14</sup>

Cesium with purity of 99.95% was obtained from Wakoh Pure Chemicals, Ind. Ltd. As Cs is a very reactive material, a lot of attention was paid to handling. The inside of the diamond cell was filled with dehydrated silicone oil, and the molten Cs in a syringe was injected into the gasket hole. The color of Cs thus enclosed in the gasket hole was golden. The formation of Cs oxide was not detected in x-ray photographs. Pressure was determined by the ruby fluorescence technique.<sup>15</sup> The pressure distribution in the sample was estimated to be less than 0.5 GPa at 8.0 GPa, judging from the broadening of the ruby line.

X-ray diffraction photographs of compressed Cs were taken to check the homogeneous distribu-